Influence of Hydrophilicity on Orientational Dynamics and Structures of Imidazolium-Based Ionic Liquid/Water Binary Mixtures

Heather E. Bailey[a], Yong-Lei Wang[a] and Michael D. Fayer*
Department of Chemistry
Stanford University, Stanford, CA 94305
*Phone: 650 723-4446, fayer@stanford.edu
[a] Heather E. Bailey and Yong-Lei Wang contributed equally to this work

Supporting Information

I. Synthesis and Characterization of 1-Ethylimidazolium tetrafluoroborate

A schematic of the synthesis of 1-ethylimidazolium tetrafluoroborate (EhimBF$_4$) is shown below in Figure S1. This procedure is based on the methods described previously by Wu[1] and Burrell.[2] Significant purification was completed via charcoal filtration[3] and ether washes. Extensive drying measures were undertaken due to extreme hydrophilic nature of ionic liquids. Karl Fischer titration (Mettler Toledo) showed that the final product has 15 ppm water. Additional characterization of EhimNTf$_2$ was completed via thermogravimetric analysis (TGA) and NMR spectroscopy.

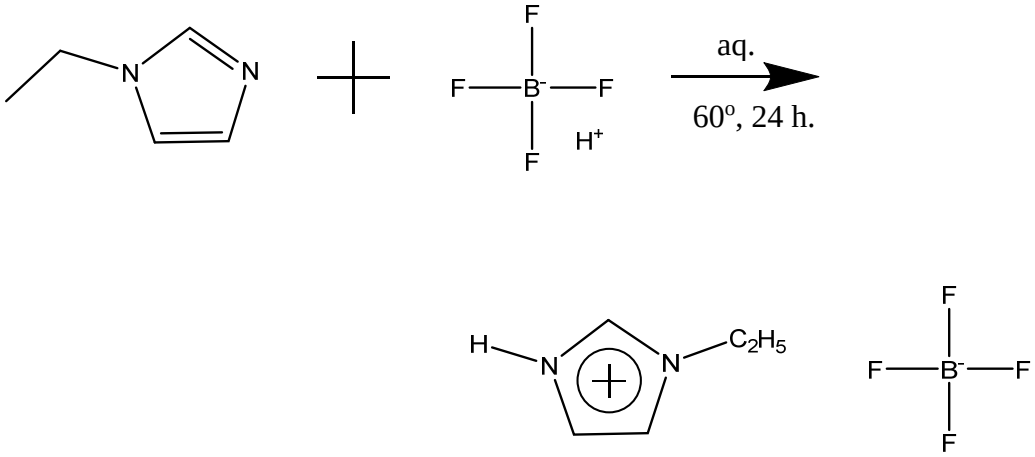

Figure S1. Schematic of synthesis of 1-ethylimidazolium tetrafluoroborate (EhimBF$_4$.)

The TGA data is presented in Figure S2. The TGA data show one drop which indicates that the product is pure since it all combusts at the same temperature. This means that the reaction went to completion. To identify the product and further determine its purity, ^{1}H NMR was used with deuterated dimethyl sulfoxide (DMSO) as solvent. The ^{1}H NMR spectrum accounted for all distinct protons in the ionic liquid, and an N-H peak was clearly observed. Additionally, minimal impurity peaks are observed which further confirms the high purity of the product.

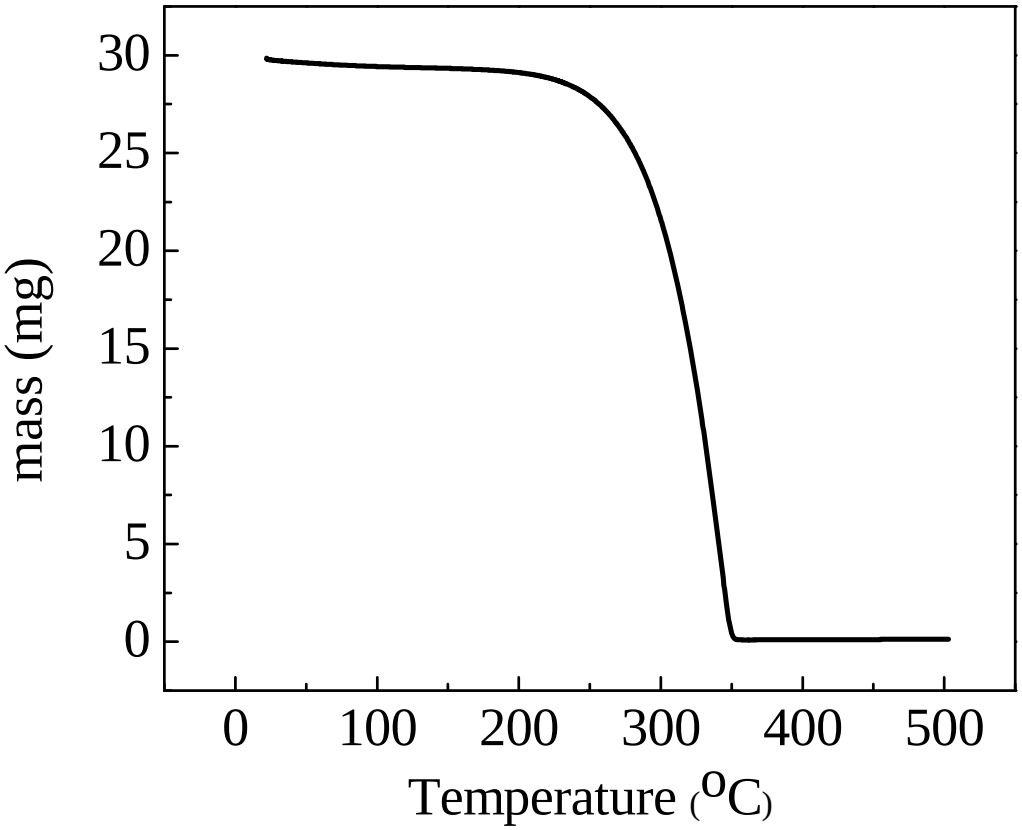

Figure S2. TGA data for $EhimBF_4$. Since the plot shows one drop, the substance is pure.

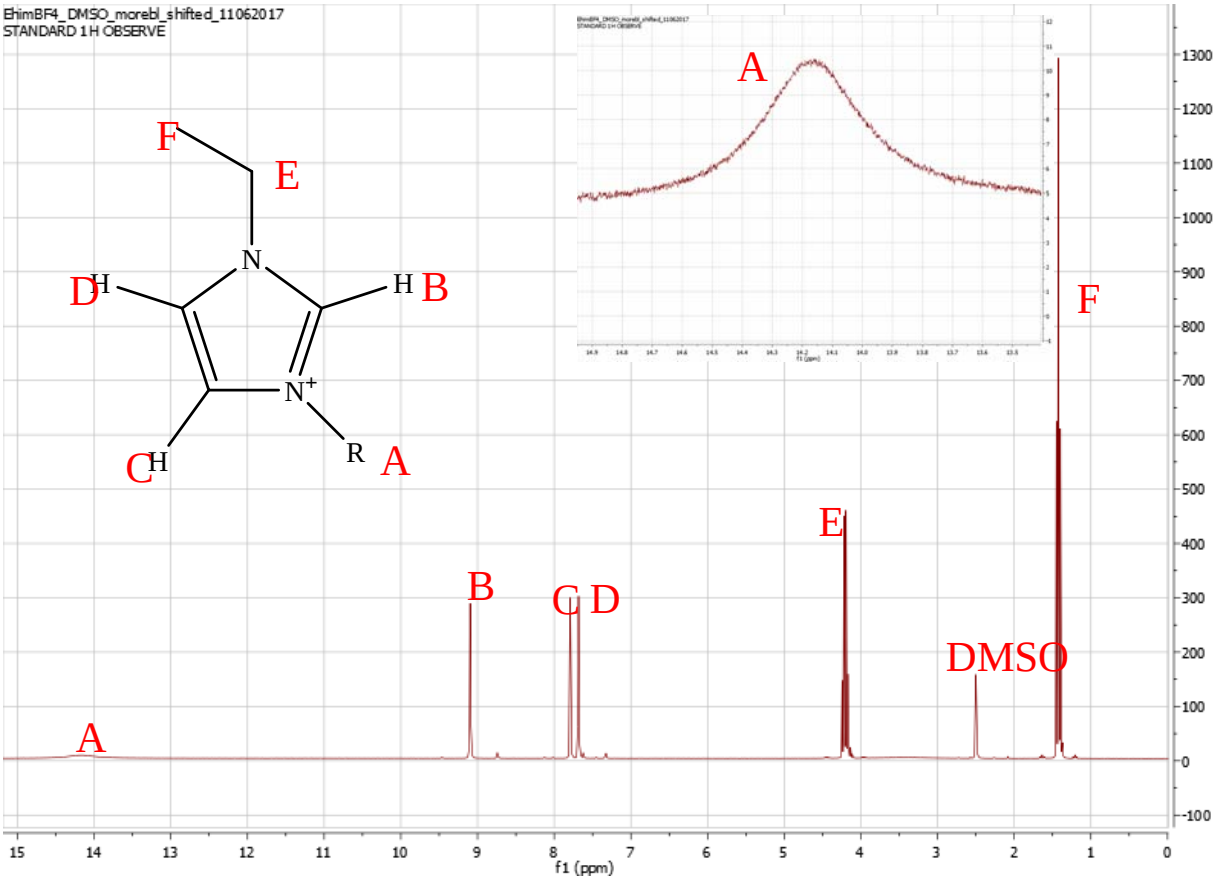

Figure S3. The ^{1}H NMR spectrum of EhimBF$_4$ in DMSO. The peaks are assigned to each set of protons in ionic liquid. An inset is include to make peak A (the broad N-H peak) easier to observe.

II. OHD-OKE fits

Additional OHD-OKE fits are shown in red in Figure S4. They are of similar quality to the OHD-OKE fits shown in the main text.

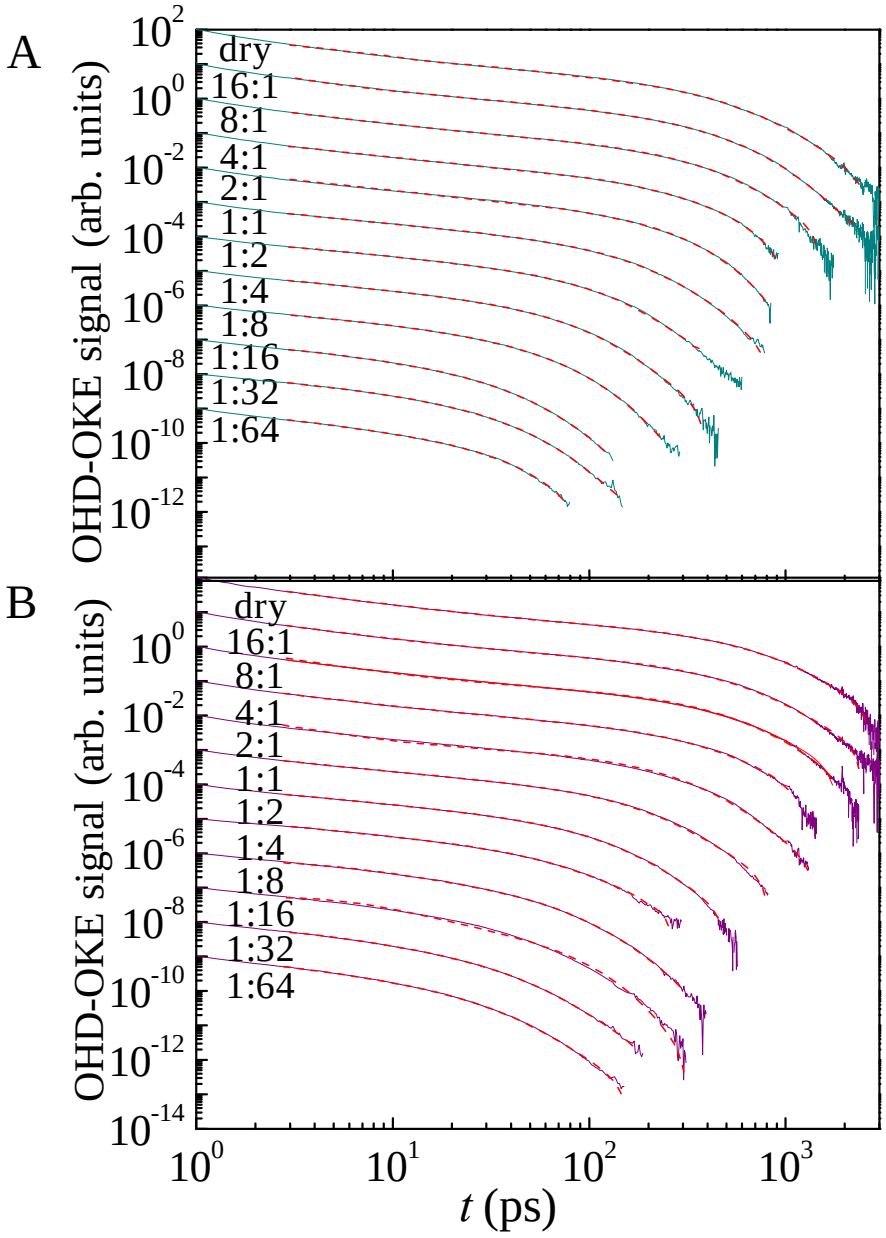

Figure S4. Additional OHD-OKE fits for (A) $EmimBF_4$ and (B) $EhimBF_4$. The fits are shown as red dashed lines over the OHD-OKE data.

III. Representative RDFs in RTIL/water mixtures

The following figures presents representative RDFs for cation-anion (Figure S5), cation-water (Figure S6), anion-water (Figure S7), and water-water (Figure S8) pairs in RTIL/water mixtures with varied water concentrations. Their significance are discussed in the main text in conjunction with the RDFs shown in Figures 9 and 10.

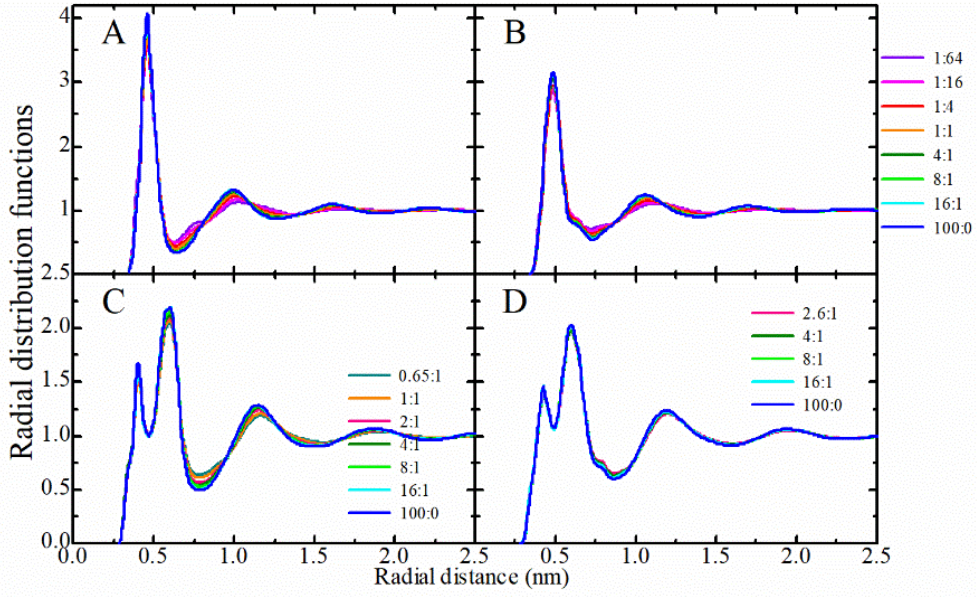

Figure S5. Radial distribution functions of cation-anion pairs in RTIL/water mixtures with varied RTIL:water ratios. (A) EhimBF$_4$, (B) EmimBF$_4$, (C) EhimNTf$_2$, and (D) EmimNTf$_2$.

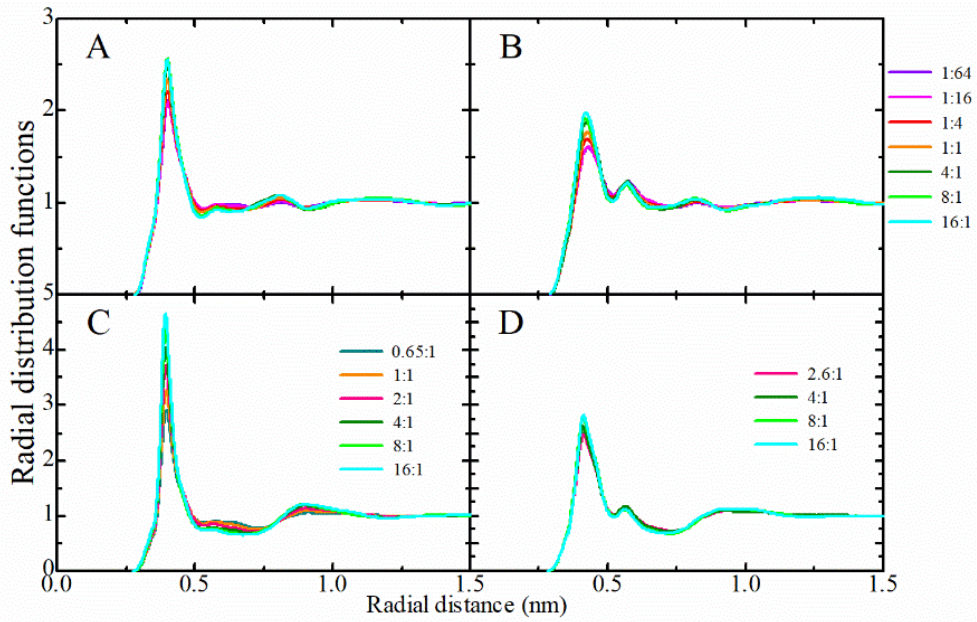

Figure S6. Radial distribution functions of cation-water pairs in RTIL/water mixtures with varied IL:water ratios. (A) $EhimBF_4$, (B) $EmimBF_4$, (C) $EhimNTf_2$, and (D) $EmimNTf_2$.

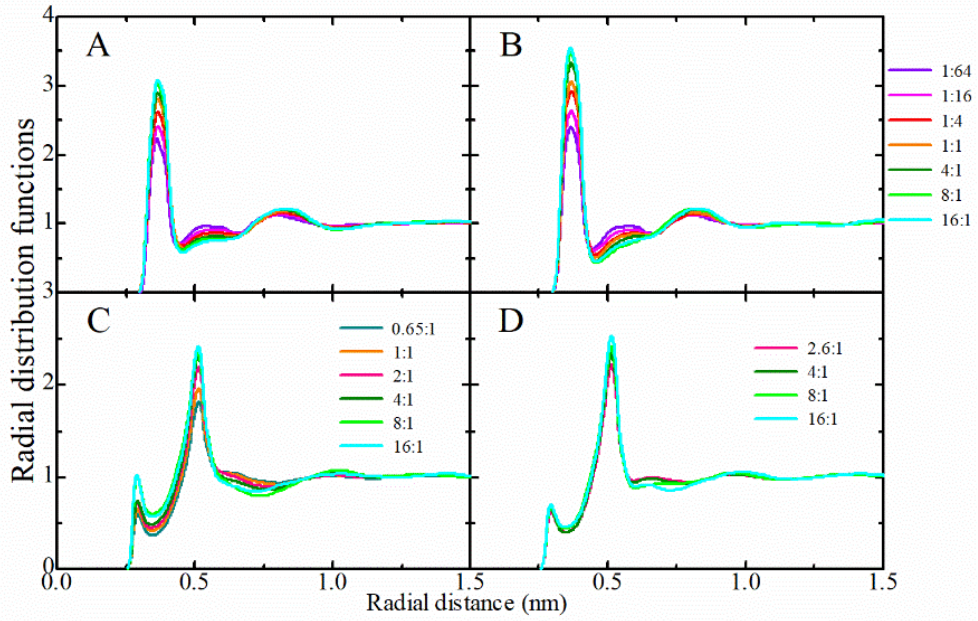

Figure S7. Radial distribution functions of anion-water pairs in RTIL/water mixtures with varied RTIL:water ratios. (A) $EhimBF_4$, (B) $EmimBF_4$, (C) $EhimNTf_2$, and (D) $EmimNTf_2$.

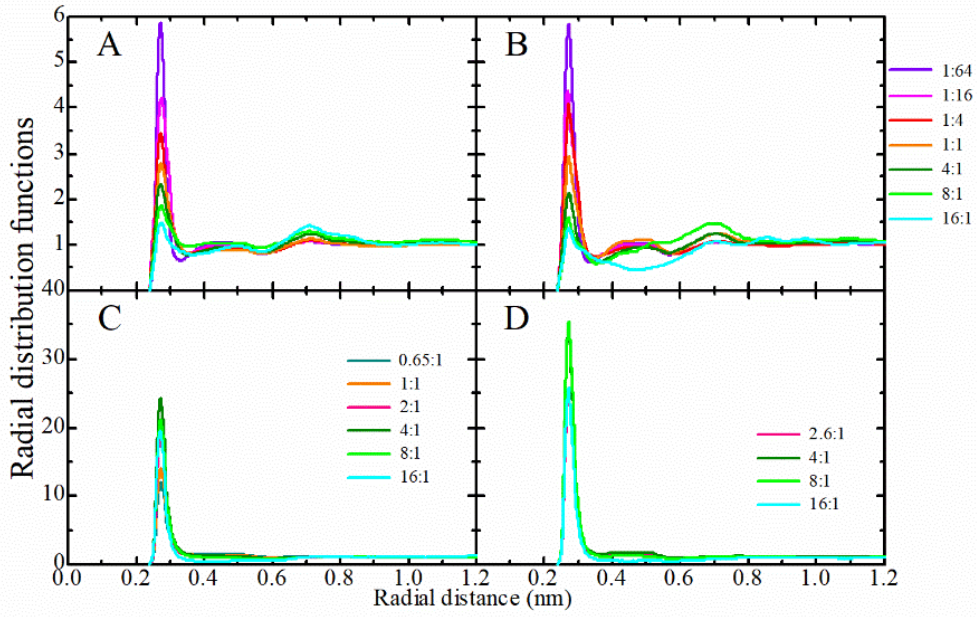

Figure S8. Radial distribution functions of water-water pair in RTIL/water mixtures with varied RTIL:water ratios. (A) $EhimBF_4$, (B) $EmimBF_4$, (C) $EhimNTf_2$, and (D) $EmimNTf_2$.

IV. Reorientational dynamics of imidazolium ring planes in RTIL/water mixtures

Figure S9 presents the second-rank Legendre polynomial $P_2(t) = \langle \bar{e}(0)\bar{e}(t) \rangle$ reorientational correlation functions of the normal vector $\bar{e}$ to the center-of-mass of the imidazolium ring planes in RTIL/water mixtures with varied water concentrations.

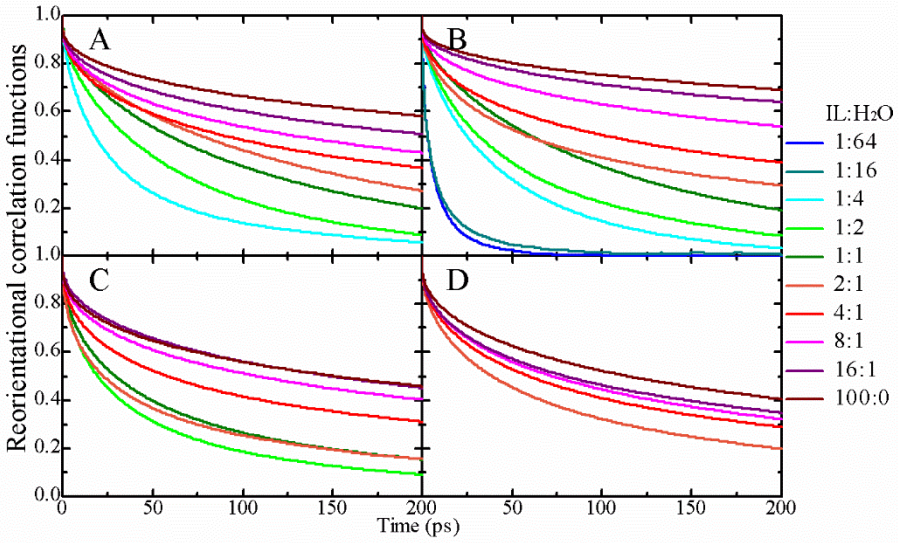

Figure S9. Reorientational correlation functions of imidazolium ring planes in RTIL/water mixtures with varied RTIL:water ratios. (A) $EhimBF_4$, (B) $EmimBF_4$, (C) $EhimNTf_2$, and (D) $EmimNTf_2$.

The parameters from the fits of this data are shown in Tables S1-S4.

Table S1 Fitting data for $EhimBF_4$

RTIL:H_2O	c_0	c_1	τ_1	c_2	τ_2
1:4	0.0011	0.48	15.9	0.41	91.7
1:2	0.0007	0.32	27.1	0.57	108.1
1:1	-0.0008	0.30	42.33	0.58	185.1
2:1	-0.0005	0.38	75.7	0.47	291.5
4:1	0.063	0.36	63.2	0.41	531.7
8:1	0.070	0.33	82.1	0.42	746.3
16:1	0.10	0.30	106.8	0.43	959.9
Dry RTIL	0.17	0.26	119.1	0.42	1327.2

Table S2 Fitting data for $EmimBF_4$

RTIL:H_2O	c_0	c_1	τ_1	c_2	τ_2
1:64	0.0000	0.47	3.34	0.38	16.5
1:16	0.0045	0.51	4.11	0.30	26.0
1:4	0.0030	0.2250	12.9423	0.6756	64.2

1:2	-0.0057	0.3232	19.6525	0.5859	105.8
1:1	0.0000	0.2226	33.2051	0.6707	159.7
2:1	0.0978	0.3201	29.2422	0.4485	243.9
4:1	0.1056	0.2635	34.9695	0.5004	357.23
8:1	0.2349	0.2115	54.7079	0.4305	541.3
16:1	0.3276	0.1711	80.5957	0.3874	713.8
Dry RTIL	0.3494	0.1477	83.5239	0.3983	9812.0

Table S3 Fitting data for $EhimNTf_2$

RTIL:H_2O	c_0	c_1	τ_1	c_2	τ_2
0.65:1	0.0001	0.53	27.9	0.28	189.3
1:1	0.0014	0.51	42.4	0.28	302.7
2:1	0.0075	0.50	40.5	0.25	366.5
4:1	0.056	0.43	76.1	0.28	673.4
8:1	0.047	0.40	106.7	0.35	977.8
16:1	0.036	0.40	143.5	0.37	1252.2
Dry RTIL	0.032	0.39	152.9	0.36	1525.4

Table S4 Fitting data for $EmimNTf_2$

RTIL:H_2O	c_0	c_1	τ_1	c_2	τ_2
2.6:1	0.0086	0.48	50.9	0.32	340.2
4:1	0.014	0.43	64.7	0.36	508.4
8:1	0.0033	0.43	76.4	0.38	651.7
16:1	0.033	0.43	90.3	0.33	786.1
Dry RTIL	0.032	0.45	142.5	0.31	1109.1

When comparing the fitting parameters of τ_2 (as given in Tables S1-S4) to the experimental values of τ from OHD-OKE experiments (Table 1), it is clear that there is good agreement between the dynamical information extracted from atomistic simulations and OHD-OKE experiments (all samples agreed within a factor of 3). The atomistic simulations and OHD-OKE experiments have the strongest agreement at high water concentration. It is also important to consider the observables in each technique.

The OHD-OKE measures the relaxation of the collective induced polarizability anisotropy. Thus, the signal is dependent on a polarizability tensor whereas the reorientational dynamics of imidazolium ring planes in the atomistic simulations are based on a single vector. At high water concentrations, the single vector representing imidazolium cations reorientation captures the relaxation of the polarizability tensor. The reduced agreement between the simulations and the experimental results as the water concentration is reduced may indicate that the tensor nature of the OHD-OKE observable becomes more important when water is not as effectively separating constituent ions and reducing Coulombic interactions among the ions. As

discussed in the main text, the key usage of atomistic simulations is to look at the thermodynamics and microstructures of these RTIL/water systems. The quality of the atomistic simulations for these quantities was confirmed by comparing simulation results to liquid densities and the X-ray scattering measurements. These are the key comparisons that ensure the quality of thermodynamics and microstructural descriptions.

References

(1) Wu, T.; Su, S.; Gung, S.; Lin, M.; Lin, Y.; Ou-Yang, W.; Sun, I.; Lai, C. Synthesis and characterization of protic ionic liquids containing cyclic amine cations and tetrafluoroborate anion. *Journal of the Iranian Chemical Society* **2011**, *8*, 149-165.

(2) Burrell, G. L.; Burgar, I. M.; Separovic, F.; Dunlop, N. F. Preparation of protic ionic liquids with minimal water content and 15N NMR study of proton transfer. *PCCP* **2010**, *12*, 1571-1577.

(3) Burrell, A. K.; Del Sesto, R. E.; Baker, S. N.; McCleskey, T. M.; Baker, G. A. The large scale synthesis of pure imidazolium and pyrrolidinium ionic liquids. *Green Chemistry* **2007**, *9*, 449-454.